

Europium-doped barium halide scintillators for x-ray and γ -ray detections

J. Selling

Department of Physics, Faculty of Science, University of Paderborn, D-33095 Paderborn, Germany

M. D. Birowosuto and P. Dorenbos

Radiation Detection Matter, Faculty of Applied Sciences, Delft University of Technology, 2629 JB Delft, The Netherlands

S. Schweizer^{a)}

Department of Physics, Faculty of Science, University of Paderborn, D-33095 Paderborn, Germany and Argonne National Laboratory, Argonne, Illinois 60439

(Received 20 September 2006; accepted 20 November 2006; published online 1 February 2007)

Single crystals of undoped or europium-doped barium chloride, bromide, and iodide were investigated under x-ray and γ -ray excitations. The Eu^{2+} -related x-ray excited luminescence found in the Eu-doped barium halides occurs at 402, 404, and 425 nm for the chloride, bromide, and iodide, respectively. $\text{BaCl}_2:\text{Eu}^{2+}$ shows the best scintillation properties of the systems investigated. The light yield is about $20\,000 \pm 2000$ photons per MeV of absorbed γ -ray energy, the energy resolution for the 662 keV photopeak is $8.8\% \pm 0.9\%$, and the scintillation decay time is 390 ± 40 ns. © 2007 American Institute of Physics. [DOI: [10.1063/1.2432306](https://doi.org/10.1063/1.2432306)]

I. INTRODUCTION

Research of scintillators has become very important during the last 20 years because of their use in x-ray radiography for medical diagnosis, nondestructive testing, and many fields of physics and chemistry. For all applications the detection of the x rays can be achieved by an x-ray scintillator. Common scintillators are based on inorganic materials.

Fluorozirconate-based glass ceramics activated with europium represent a promising class of x-ray scintillators.^{1,2} In contrast to common single-crystal scintillators, glass ceramics can be manufactured easily in any size and shape. The scintillation in these glass ceramics is mainly caused by the $5d-4f$ transition of europium(II) incorporated in barium chloride nanocrystals that are formed in the glass matrix upon appropriate thermal processing. To better understand the scintillation properties in europium-activated barium halide nanocrystals in general, an investigation of the processes in the corresponding bulk material is essential.

Typical performance characteristics for scintillators are energy resolution, light yield, and scintillation decay time. The energy resolution indicates the relation of the light output to the energy of the penetrating gamma quantum. The light yield is the fast part of the generated light after the absorption of an energetic photon (x-ray or gamma quantum) obtained from pulse height spectra; integrated x-ray excited luminescence spectra provide information on the integral scintillation efficiency. A fast scintillation decay time is necessary for fast-timing or high-count-rate applications.

II. EXPERIMENTAL TECHNIQUES

A. Sample preparation and crystal structure

Undoped and Eu-doped single crystals of orthorhombic BaX_2 ($X=\text{Cl}$, Br , and I) were grown in the University of

Paderborn crystal growth laboratory using the Bridgman method. To prepare the Eu-doped samples, BaX_2 powder was added to 1000 molar ppm of EuX_2 in a quartz glass ampoule with a SiX_4 atmosphere. Prior to crystal growth the BaX_2 powder was dried in vacuum with subsequent melting in the SiX_4 atmosphere to reduce oxygen contamination. However, the silicon treatment did not work for the BaI_2 powder. The usual technique was completed by slow cooling through the cubic-orthorhombic phase transition near 920°C for BaCl_2 (Ref. 3) and 800°C for BaBr_2 .⁴

The stable phase of BaX_2 crystals at room temperature (RT) has the orthorhombic PbCl_2 structure characterized by the space group D_{2h}^{16} ($Pnma$).³ The lattice parameters, density, and effective Z are summarized in Table I. The rare-earth dopant Eu^{2+} is substituted at Ba^{2+} sites having nine halide ions as close neighbors at slightly varying distances.

B. Experimental setup

The x-ray excited luminescence (XL) and afterglow spectra were recorded at the University of Paderborn using a 0.22 m double monochromator (Spex) in combination with a cooled photomultiplier (Hamamatsu R943-02) working in single-photon counting mode (HP 5370B universal time interval counter). All spectra were recorded at RT and not corrected for spectral sensitivity of the experimental setup. The x-ray irradiation was carried out with a mobile x-ray tube (Phillips MGC 01) using a tungsten anode at 60 kV and 15 mA.

Pulse height spectra were obtained at the Delft University of Technology with a Hamamatsu R1791 photomultiplier tube (PMT) with a box-type dynode structure connected to a preamplifier and an Ortec 672 spectroscopy amplifier inside an M-Braun Unilab dry box. The crystals were mounted directly to the window of the PMT and covered with several Teflon layers to optimize the light collection. The photoelectron yield (LY_{phe} in photoelectrons per MeV)

^{a)}Author to whom correspondence should be addressed; electronic mail: stefan.schweizer@uni-paderborn.de

TABLE I. Lattice parameters (Ref. 3), density (Ref. 5), and effective Z (for energies between 100 keV and 1 MeV) (Ref. 6) of BaX_2 .

| Crystal | a (Å) | b (Å) | c (Å) | Density (g/cm ³) | Effective Z |
|-------------------|------------|------------|------------|---------------------------------|---------------|
| BaCl ₂ | 7.865 | 4.731 | 9.421 | 3.888 | 49.8 |
| BaBr ₂ | 8.276 | 4.956 | 9.919 | 4.781 | 47.8 |
| BaI ₂ | 8.922 | 5.304 | 10.695 | 5.15 | 54.1 |

is obtained by comparing the peak position of the photopeak with that of the single-electron spectrum.⁷ The absolute light yield, LY_{ph} in photons per MeV (photons/MeV), is derived from LY_{phe} as follows:⁸

$$LY_{ph} = (1 - R_{eff}) / (0.98 \cdot QE_{eff}) \cdot LY_{phe}. \quad (1)$$

The effective quantum efficiency QE_{eff} of the PMT was obtained from the manufacturer, and the PMT effective reflectivity R_{eff} was measured. Both are averaged over the spectral profile of the γ -ray excited scintillation spectrum. The position as well as the energy resolution of the photopeak (full width at half maximum) was determined by fitting the photopeak with a Gaussian curve.

The scintillation decay time was measured at Delft University of Technology. The spectra were recorded by two methods. The first is the single-photon counting technique described by Bollinger and Thomas.⁹ For this method, scintillation decay time spectra can be recorded up to a maximum time range of 200 μ s with XP2020Q PMTs, Ortec 934 constant fraction discriminators, Ortec 567 time-to-amplitude converter (TAC), and AD513A CAMAC analog-to-digital converter (ADC). The time ranges used for measurements presented in this work vary from 10 to 20 μ s.

For recording decay time spectra at longer times than 200 μ s, the multihit method¹⁰ was used. The TAC and ADC in the single-photon counting technique were replaced by a Lecroy 4208 time-to-digital converter (TDC) having a channel width of 1 ns. By this method, the short decay component and its contribution to the total light yield are less accurately obtained than those by the single-photon counting technique.

III. EXPERIMENTAL RESULTS

A. X-ray excited luminescence and integral scintillation efficiency

Figure 1 shows the normalized XL spectra of undoped and Eu-doped BaCl₂, BaBr₂, and BaI₂. The XL of undoped BaCl₂ shows a broad band at about 300 nm and a double-peak structured band between 380 and 600 nm with maxima at 420 and 475 nm. The ultraviolet XL band at about 300 nm can only be seen in undoped BaCl₂ but not in any of the other samples. The XL of undoped BaBr₂ shows a similar double-peak structured band as found in undoped BaCl₂ with peak positions at 425 and 475 nm. However, the intensity ratio of the 425 to the 475 nm band has changed in favor of the longer wavelength. In undoped BaI₂ a broad XL band at about 530 nm with a small shoulder at about 430 nm can be found.

TABLE II. Light yields and XL-to-afterglow ratios of undoped and Eu-doped barium halides. The light yield was derived by comparing the integrated area under the XL curve of the corresponding barium halide to that of a CdWO₄ [28 000 photons/MeV (Ref. 11)] reference sample. The XL-to-afterglow ratio was detected at the wavelengths indicated.

| Crystal | Integral scintillation efficiency with respect to CdWO ₄ (photons/MeV) | XL-to-afterglow ratio (after 3 s) |
|-----------------------|---|--------------------------------------|
| BaCl ₂ | 4 500±500 | 20% at 420 nm 25% at 475 nm |
| BaBr ₂ | 8 700±870 | 1% at 425 nm 2% at 475 nm |
| BaI ₂ | 1 700±170 | <0.1% |
| BaCl ₂ :Eu | 19 000±1900 | 0.2% at 402 nm |
| BaBr ₂ :Eu | 32 000±3200 | 10% at 404 nm |
| BaI ₂ :Eu | 2 000±200 | <0.1% |

The XL spectra of the Eu-doped BaCl₂ and BaBr₂ do not show any of the features described above but single bands at 402 and 404 nm, respectively. This band is due to the typical $5d-4f$ transition of Eu²⁺. The 404 nm band in BaBr₂ shows a small shoulder at about 480 nm. The Eu²⁺ emission is further shifted to longer wavelengths in Eu-doped BaI₂, where it is seen as a small peak at about 425 nm. The XL of Eu-doped BaI₂ is dominated by the broadband at 530 nm, which also appeared in undoped BaI₂. The most intense XL peak occurred for the Eu²⁺ $5d-4f$ transition in BaBr₂ followed by BaCl₂. The Eu²⁺ emission in BaI₂ is very weak.

For a rating of the scintillation properties with regard to light yield, single crystals of the undoped and Eu-doped barium halides were compared to the common scintillator CdWO₄. The measurements were made using the same parameters for all crystals. The area under the XL curve was calculated and compared to that of CdWO₄.¹¹ The results are

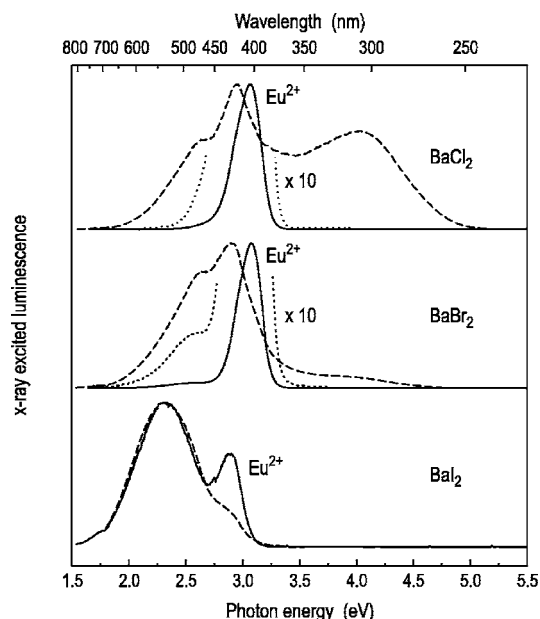


FIG. 1. Normalized x-ray excited luminescence spectra of undoped (dashed curves) and Eu-doped (solid curves) barium halides. Parts of the spectra of the Eu-doped samples (dotted curves) are blown up ten times as indicated. All spectra were recorded at RT.

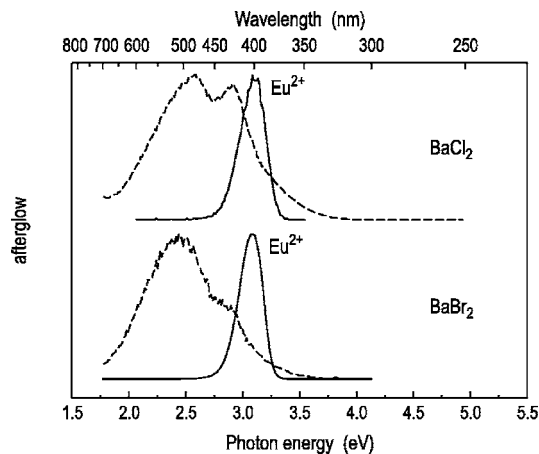


FIG. 2. Normalized afterglow spectra of undoped (dashed curves) and Eu-doped (solid curves) barium halides. All spectra were recorded at RT.

given in Table II. The integral scintillation efficiencies of the Eu-doped samples are reported in Ref. 12. The value for $\text{BaI}_2:\text{Eu}^{2+}$ presented in Table II is slightly larger than in Ref. 12.

B. Afterglow

Figure 2 shows the normalized afterglow spectra of undoped and Eu-doped BaCl_2 and BaBr_2 . The afterglow of undoped and Eu-doped BaI_2 was too weak to allow the recording of the spectral behavior. The afterglow spectra of the Eu-doped samples (Fig. 2, solid curves) are almost identical to the corresponding XL spectra. The spectra are dominated by the Eu^{2+} emissions at 402 and 404 nm for BaCl_2 and BaBr_2 , respectively. The afterglow spectrum of the undoped BaCl_2 does not show the broad 300 nm luminescence band found in XL but the double-structured band with peaks at 420 and 475 nm. However, the intensity ratio of the 420 to the 475 nm band has changed in favor of the longer wavelength. For undoped BaBr_2 the situation is similar: The afterglow spectrum shows the same double-structured band as already observed in XL, with an intensity ratio in favor of the longer wavelength. In both cases, the change in the intensity ratio is caused by the slightly higher afterglow intensity of the longer wavelength. This finding was confirmed by measurements on the temporal behavior of the XL/afterglow intensity.

Figure 3 shows the temporal behavior of the XL/afterglow intensity of undoped and Eu-doped barium halides after switching on (for 5 min) and off the x-ray excitation at RT; the resolution of these measurements was 3 s, i.e., every 3 s a data point was recorded. Undoped BaCl_2 shows an afterglow in the range from 20% (420 nm) to 25% (475 nm). The Eu^{2+} emission in BaCl_2 has an afterglow of about 0.2%. In contrast to BaCl_2 , the afterglow of undoped BaBr_2 is less than that of the Eu-doped sample: The Eu^{2+} emission has an afterglow of 10%, while the afterglow in undoped BaBr_2 ranges from 1% (425 nm) to 1.5% (475 nm). Undoped and Eu-doped BaI_2 show an afterglow below 0.1%. The XL-to-afterglow ratios detected at the wavelengths indicated are listed in Table II.

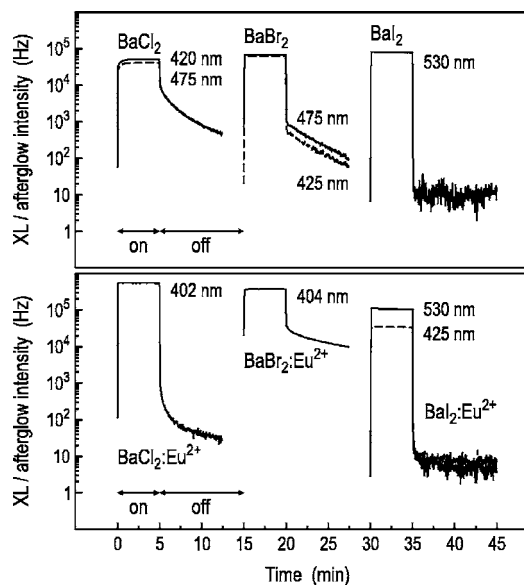


FIG. 3. Temporal behavior of the XL/afterglow intensity of undoped and Eu-doped barium halides after switching on and off the x-ray excitation at RT; the XL/afterglow intensity was detected at the wavelength indicated.

C. Light yield and energy resolution

Light yields and energy resolution for the undoped and Eu-doped barium chlorides and bromides were derived from pulse height spectra under 662 keV γ -ray excitation of a ^{137}Cs source; the spectra are shown in Fig. 4. To determine the position of the photopeak and the energy resolution, the photopeaks were fitted by Gaussian curves. Besides the photopeak at 662 keV, the spectra show the Compton continuum from the Compton edge at about 450 keV down to zero energy. The backscatter peak, which arises from scattering of the γ rays from the photomultiplier and materials outside the system back into the scintillation crystals, is at 200 keV. The leftmost peak at 32 keV corresponds to the $K\alpha$ x rays of barium, which are also emitted in a ^{137}Cs decay. The unusual

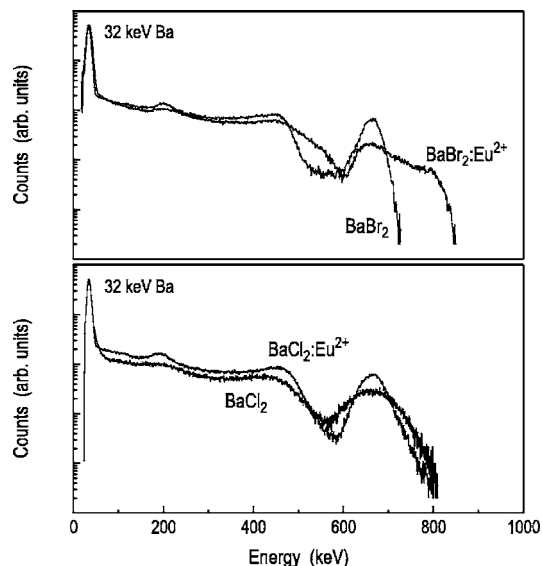


FIG. 4. Pulse height spectra of undoped and Eu-doped barium bromides and chlorides under a 662 keV γ -ray excitation of a ^{137}Cs source. The spectra are measured with a shaping time of 10 μs at RT.

TABLE III. Light yield, energy resolution, and scintillation decay of undoped and Eu-doped barium halides. The light yield and energy resolution values for $\text{BaCl}_2:\text{Eu}^{2+}$ and $\text{BaBr}_2:\text{Eu}^{2+}$ were derived from pulse height spectra (shaping time of $10\ \mu\text{s}$) under a $662\ \text{keV}$ γ ray excitation of a ^{137}Cs source; the values for $\text{BaI}_2:\text{Eu}^{2+}$ were obtained from pulse height spectra under $59.9\ \text{keV}$ γ rays of a ^{241}Am source. The scintillation decay measurements for the BaCl_2 and BaBr_2 crystals were carried out with the single-photon counting method, those for the BaI_2 crystals with the multihit method. For the fitting of the BaI_2 decay curves, the second component was kept constant.

| Crystal | Light yield (photons/MeV) | | Energy resolution (%) | Scintillation decay time (ns) |
|---------------------------|------------------------------|--------------------|--------------------------|-------------------------------------|
| | $0.5\ \mu\text{s}$ | $10\ \mu\text{s}$ | | |
| BaCl_2 | $1\ 500 \pm 150$ | $1\ 700 \pm 150$ | 17.4 ± 1.7 | 980 ± 100 (100%) |
| $\text{BaCl}_2:\text{Eu}$ | $14\ 400 \pm 1450$ | $19\ 400 \pm 1950$ | 8.8 ± 0.9 | 390 ± 40 (100%) |
| BaBr_2 | $5\ 100 \pm 500$ | $19\ 300 \pm 1950$ | 5.4 ± 0.5 | 2200 ± 220 (100%) |
| $\text{BaBr}_2:\text{Eu}$ | $10\ 800 \pm 1100$ | $15\ 700 \pm 1550$ | 11.0 ± 1.1 | 585 ± 60 (100%) |
| BaI_2 | $1\ 100 \pm 100$ | $2\ 600 \pm 250$ | ... | 610 ± 50 (65%), 5000 (const) |
| $\text{BaI}_2:\text{Eu}$ | $2\ 300 \pm 250$ | $3\ 800 \pm 400$ | ... | 510 ± 50 (80%) 5000 (const) |

broadening of the photopeak in $\text{BaBr}_2:\text{Eu}^{2+}$ is probably caused by inhomogeneities in the crystal. The values for the undoped and Eu-doped barium iodides were obtained from pulse height spectra under $59.9\ \text{keV}$ γ rays of a ^{241}Am source (the spectra are not shown); the barium iodides did not show any photopeak under a $662\ \text{keV}$ γ -ray excitation. Light yields and the energy resolution of undoped and Eu-doped barium halides are compiled in Table III.

Of all the barium halides studied, undoped BaBr_2 and $\text{BaCl}_2:\text{Eu}^{2+}$ show the highest light yield with $19\ 300 \pm 1950$ and $19\ 400 \pm 1950$ photons/MeV, respectively. The values were obtained with a shaping time of $10\ \mu\text{s}$. Increasing the shaping time from 0.5 to $10\ \mu\text{s}$ leads to an increase in the light yield of more than 70% for undoped BaBr_2 . This change indicates a slow scintillation component in the microsecond range. The increases in the light yield in Eu-doped BaCl_2 and BaBr_2 are 25% and 30%, respectively. For undoped BaCl_2 , which shows the lowest yield light of all samples, only a weak increase—meaning a fast scintillation component—is found upon increasing the shaping time from 0.5 to $10\ \mu\text{s}$. The undoped and Eu-doped barium iodides show an increase of almost 200%.

D. Scintillation decay

In Fig. 5 the scintillation decay curves of undoped and Eu-doped barium halides are presented. All samples were measured with TDC and TAC. The results of the two methods correspond with each other within an error of 10%. The curves for BaCl_2 and BaBr_2 were measured with the single-photon counting method, whereas those for the BaI_2 samples were measured with the multihit method. The scintillation decay components are collected in the last column of Table III. The decay components for Eu-doped BaCl_2 and BaBr_2 are much faster than those observed for the corresponding undoped sample, whereas both undoped and Eu-doped BaI_2 show about the same temporal behavior. The emission in

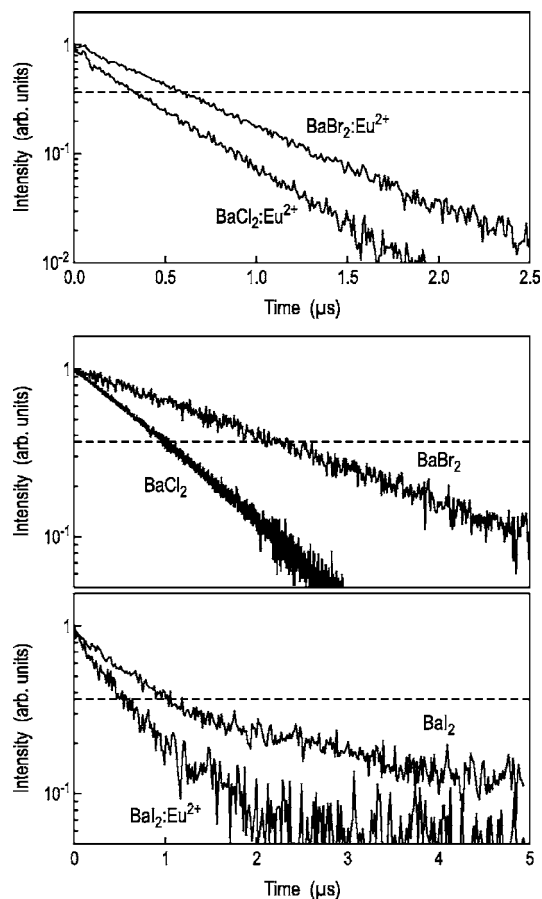


FIG. 5. Normalized scintillation decay curves of undoped and Eu-doped barium halides under a $662\ \text{keV}$ γ -ray excitation of a ^{137}Cs source. The measurements for the BaCl_2 and the BaBr_2 crystals were carried out with the single-photon counting method, those for the BaI_2 crystals with the multihit method. All decay curves were recorded at RT.

BaI_2 is dominated by the $530\ \text{nm}$ band, and its decay can be fitted by assuming two different components.

IV. DISCUSSION

The x-ray excited Eu^{2+} emission in Eu-doped barium halides (solid curves in Fig. 1) shifts from chloride to iodide to longer wavelengths. For Eu-doped BaCl_2 and BaBr_2 the Eu^{2+} emission dominates the XL spectrum; the double-structured XL band at about $450\ \text{nm}$ observed in the undoped samples cannot be seen in Eu-doped BaCl_2 , but it is found as a small shoulder in the case of Eu-doped BaBr_2 (Fig. 1, dotted curves). The XL band at $530\ \text{nm}$ in undoped BaI_2 is also present in the XL spectrum of Eu-doped BaI_2 and is even more intense than the Eu-correlated emission at $425\ \text{nm}$. The $450\ \text{nm}$ XL found in undoped BaBr_2 has previously been ascribed to $F-V_K$ center recombination.¹³ The $450\ \text{nm}$ band in undoped BaCl_2 and the $530\ \text{nm}$ band in BaI_2 might be caused by the same process. We assume that there is an energy transfer mechanism between the $F-V_K$ pair and Eu^{2+} . This transfer is very efficient in the case of BaCl_2 , efficient in the case of BaBr_2 , but almost completely suppressed in the case of BaI_2 . The reason for this is still unclear. At this point, we cannot say much about the scintillation mechanism in the barium halides investigated because

dedicated experiments, such as decay time and light yield measurements (as a function of temperature and concentration), were not performed.

The aim of this paper was to explore whether the materials studied can be interesting scintillator candidates. The best scintillator of the barium halides investigated—with respect to light yield, scintillation decay time, and afterglow—is Eu-doped BaCl₂. The light yield is 19 400 photons/MeV (see Table III), the scintillation decay consists of a fast component on the submicrosecond scale (about 400 ns, see Table III), and the afterglow is less than 0.2% (see Table II). Moreover, the energy resolution under the 662 keV γ -ray excitation of a ¹³⁷Cs source is 8.8%.

Although undoped BaBr₂ is also a good scintillator in terms of the light yield (19 300 photons/MeV, see Table III), its scintillation decay component is on the multiple microsecond scale (2200 ns, see Table III), which makes this system less attractive for scintillation applications. The XL-to-afterglow ratio of undoped BaBr₂ is 1%–2%; the energy resolution is 5.4% and thus slightly better than that of Eu-doped BaCl₂.

At first glance, a comparison between the light yield values obtained from the pulse height spectra (see Table III) and those from the XL spectra (see Table II), which were compared to CdWO₄ [28 000 photons/MeV (Ref. 11)], shows that some of the data do not agree with each other. An explanation for this discrepancy lies in the recording method of the data. The light yield values derived from the pulse height spectra were recorded with a maximal shaping time of 10 μ s, whereas each data point of the XL spectra was obtained after 1–2 s of integration and was thus additionally increased by afterglow effects. The light yield values in Table III agree with those in Table II in the case of low afterglow samples, e.g., Eu-doped BaCl₂. Samples having an intense afterglow such as undoped BaCl₂ and Eu-doped BaBr₂ show in the XL spectra a much higher light yield, leading to a higher value in Table II. The XL light yield values for the undoped and Eu-doped BaI₂ are smaller than those of the pulse height spectra values. BaI₂ is very hygroscopic and becomes opaque while performing the XL measurements; the light yield thus decreases. For the pulse

height spectra, the measurements were performed inside an M-Braun Unilab dry box with a moisture content less than 1 ppm. Finally, one may not exclude a nonproportional response of the scintillators with energy of excitation. Usually, scintillators are less efficient at x-ray energies (10–50 keV) than at gamma-ray energy (662 keV), and this may also contribute to differences between the x-ray light yield in Table II and the γ -ray light yield in Table III.

ACKNOWLEDGMENTS

The Delft part of this work was supported by the Netherlands Technology Foundation (STW). Argonne National Laboratory is operated by the University of Chicago for the Department of Energy under Contract No. W-31-109-Eng-38.

¹G. Chen, J. A. Johnson, S. Schweizer, J. Woodford, P. Newman, and D. MacFarlane, Proc. SPIE **6142**, 61422X (2006).

²J. Johnson, S. Schweizer, B. Henke, G. Chen, J. Woodford, P. Newman, and D. MacFarlane, J. Appl. Phys. **100**, 034701 (2006).

³E. B. Brackett, T. E. Brackett, and R. L. Sass, J. Phys. Chem. **67**, 2132 (1963).

⁴E. Monberg and Y. Ebisuzaki, J. Cryst. Growth **21**, 307 (1974).

⁵E. Lax, *D'Ans-Lax: Taschenbuch für Chemiker und Physiker, Band 1* (Berlin, Heidelberg, Springer, 1967).

⁶C. W. E. van Eijk, *New Scintillators, New Light Sensors, New Applications*, in Proc. Int. Conf. on Scintillators and their Applications (SCINT 97) (Shanghai Branch Press, Shanghai, China, 1997), pp. 3–12.

⁷M. Bertolaccini, S. Cova, and C. Bussolati, *A technique for absolute measurement of the effective photoelectron per keV yield in scintillation counters*, in Proc. Nucl. Electr. Symp., Versailles, France (1968).

⁸J. T. M. de Haas, P. Dorenbos, and C. W. E. van Eijk, Nucl. Instrum. Methods Phys. Res. A **537**, 97 (2005).

⁹L. M. Bollinger and G. E. Thomas, Rev. Sci. Instrum. **32**, 1044 (1961).

¹⁰W. W. Moses, Nucl. Instrum. Methods Phys. Res. A **336**, 253 (1993).

¹¹P. Dorenbos, J. M. T. de Haas, and C. W. E. van Eijk, IEEE Trans. Nucl. Sci. **42**, 2190 (1995).

¹²J. Selling, G. Corradi, M. Secu, and S. Schweizer, *Rare-earth doped barium halide x-ray storage phosphors and scintillators*, in Proc. of the Eighth International Conference on Inorganic Scintillators and their Use in Scientific and Industrial Applications (SCINT 2005), Alushta, Crimea, Ukraine, September 19–23, 2005, edited by A. Gektin and B. Grinyov (National Academy of Sciences of Ukraine, Ukraine-Kharkov, 2006), pp. 415–418.

¹³M. Secu, S. Schweizer, U. Rogulis, and J.-M. Spaeth, J. Phys.: Condens. Matter **15**, 2061 (2003).